Published in final edited form as:
Anal Bioanal Chem. 2011 October ; 401(6): 1881–1888. doi:10.1007/s00216-011-5257-z.

Kinetic Analysis of PI3K Reactions with Fluorescent PIP_2 Derivatives

Weigang Huang[1], **Dechen Jiang**[2], **Xiaoyang Wang**[1], **Kelong Wang**[2], **Christopher E. Sims**[2], **Nancy L. Allbritton**[2,3], and **Qisheng Zhang**[1,*]

[1]Division of Medicinal Chemistry & Natural Products, University of North Carolina at Chapel Hill, Chapel Hill, NC 27599

[2]Department of Chemistry, University of North Carolina at Chapel Hill, Chapel Hill, NC 27599

[3]Department of Biomedical Engineering, University of North Carolina, Chapel Hill, NC 27599 and North Carolina State University, Raleigh, NC 27695

Abstract

PI3K signaling plays important roles in cell differentiation, proliferation, and migration. Increased mutations and expression levels of PI3K are hallmarks for the development of certain cancers. Pharmacological targeting of PI3K activity has also been actively pursued as a novel cancer therapeutic. Consequently, measurement of PI3K activity in different cell types or patient samples holds the promise as being a novel diagnostic tool. However, the direct measurement of cellular PI3K activity has been a challenging task. We report here the characterization of two fluorescent PIP_2 derivatives as reporters for PI3K enzymatic activity. The reporters are efficiently separated from their corresponding PI3K enzymatic products through either thin layer chromatography (TLC) or capillary electrophoresis (CE), and can be detected with high sensitivity by fluorescence. The biophysical and kinetic properties of the two probes are measured, and their suitability to characterize PI3K inhibitors is explored. Both probes show similar capacity as PI3K substrates for inhibitor characterization, yet also possess distinct properties that may suggest their different applications. These characterizations have laid the groundwork to systematically measure cellular PI3K activity, and have the potential to generate molecular fingerprints for diagnostic and therapeutic applications.

Keywords

PI3K assay; fluorescent phosphatidylinositides; TLC analysis; capillary electrophoresis

1. Introduction

Phosphatidylinositides (PIs) are not only integral components of cell membranes, but also among the most versatile endogenous signaling molecules [1]. Dynamic changes of PIs in the membranes, particularly phosphatidylinositol 4,5-bisphosphate (PIP_2) and phosphatidylinositol 3,4,5-trisphosphate (PIP_3), are fundamental to many functional processes including cell proliferation and migration [2]. Phosphatidylinositol 3-kinase (PI3K) catalyzes the phosphorylation of PIP_2 to form PIP_3 (Fig. 1A), while phosphatase and tensin homolog (PTEN) dephosphorylates PIP_3 to regenerate PIP_2. Dysfunction of either PI3K or PTEN has been linked to various diseases including cancer and diabetes [3–5]. For example, the somatic mutation or amplification of PI3K has been found in breast, colorectal,

qszhang@unc.edu.

glioblastoma, and pancreatic cancer [6–7]. Consequently, small molecule PI3K inhibitors have been actively pursued by pharmaceutical companies, and a number of compounds are in clinical trials in oncology [8–10].

Although PI3K mutation and amplification have been firmly linked to various diseases, whether and how genetic changes quantitatively impact enzymatic activity has not been well established. This is partly due to the lack of suitable reporters and analytical tools to directly measure cellular PI3K activity. Among the known methods for PI3K activity measurement, radioactivity-based assays have been the most widely used [11]. In these methods, the cells are metabolically labeled with radioactive materials extracted with organic solvents. The lipid fraction is separated by thin-layer chromatography (TLC) or high performance liquid chromatography (HPLC) and detected by autoradiography. This approach has the advantage of yielding quantitative results, and can be optimized to differentiate various lipids. However, the assays are subject to cell-dependent differences in steady-state PI metabolism and variable expression of PI3K. In addition, the incorporation efficiency of the radioactive material may be low, and the sensitivity and specificity of the incorporation are limited. To avoid metabolic labeling, matrix-assisted laser desorption ionization mass spectrometry (MALDI-MS) has gained popularity for the rapid analysis of lipids in various biological samples [12–13]. A solvent extraction procedure of the lipids from the unpurified sample is typically carried out prior to the MALDI-MS measurements. This method distinguishes different lipids by their molecular weights; however, it does not distinguish between isomers and requires sophisticated and expensive equipment. In addition, the dynamic range of lipid concentrations in the cells makes the detection of low abundance lipids very difficult. The phosphorylation of downstream proteins, such as protein kinase B (PKB, *aka* Akt), has also been used to evaluate cellular PI3K activity. However, phosphorylation of Akt is an indirect measure and confounded by the phosphorylation of Akt by other kinases. Finally, fluorescently labeled pleckstrin homology (PH) domains have been used as an indirect assay of the enzymatic activities of PI3K and PTEN. Cells are transfected with a PH domain that binds to the substrate PI of interest, and is tagged with a fluorescent protein such as green fluorescent protein (GFP) [14]. A change in membrane-associated fluorescence signal will occur if the level of the PI in the membrane changes. The major problems are that binding specificity and affinity of the PI-binding domains towards various PIs are not very high, and they are known to interact with other protein ligands. In addition, these molecularly engineered cell-based assays cannot be used in clinical samples.

For *in vitro* assays, PI3K activity can be measured by monitoring the incorporation of ^{32}P into PIP_2 to form radioactive PIP_3. In addition, PH domains have been used as detectors in measuring the production or localization of PIP_3 [15]. In a competitive assay of PI3K activity, the PIP_2 is combined with PI3K and a PH domain that specifically detects the reaction product PIP_3. The reaction mixture is then added to a plate coated with PIP_3 and the binding of the probe is detected through fluorescence polarization or luminescence to reflect the PI3K activity [16]. These assays have gained popularity because of their relative simplicity and suitability for high throughput screens, but such assays measure PI3K activity indirectly and the accuracy is affected by many factors. These various limitations require new techniques for analysis of PI3K activity directly and rapidly which can also be used in clinically relevant situations where the amount of sample, such as from a patient, is limited.

To address this need, lipids tagged with fluorophores have been developed as substrates for a variety of lipid metabolic enzymes, often with similar kinetics to the endogenous substrates [17–18]. BODIPY-tagged BODIPY-PIP_2 (Fig. 1B) and fluorescein-tagged FL-PIP_2 (Fig. 1C) have been used to image cellular localization of PIP_2 [19]. Recently, Caliper Lifesciences employed FL-PIP_2 as a PI3K substrate for an *in vitro* assay in which conversion of the FL-PIP_2 to FL-PIP_3 was monitored by electrophoretic chemical separation

with laser-induced fluorescence detection in a microfabricated fluidic chip. Such highly-sensitive, chemical separation techniques for monitoring phosphorylation lend themselves to cell-based assays, and several examples using capillary electrophoresis (CE) with fluorescent peptide- and lipid-based probes have been reported in single-cell biochemical measurements [20–21]. However, the amphiphilic nature of PI lipids renders them to potential loss on the column during CE separation. Consequently, the accuracy of PI3K activity measurement has to be validated. Toward the goal to adapt fluorescent PIP_2 derivatives to measure PI3K activity in patient samples, we carried out detailed kinetic studies using both thin layer chromatography (TLC) and capillary electrophoresis (CE) analyses.

2. Materials and Methods

Materials

Purified PI3K (PIK3CA/PIK3R1) was obtained from Invitrogen. FL-PIP_2 and FL-PIP_3 were purchased from Cayman Chemical. BODIPY-PIP_3 was purchased from Echelon Bioscience. BODIPY-PIP_2 was synthesized according to the literature protocols [22]. EOTrol LR was obtained from Target Discovery. Wortmannin, LY294002, ATP, sodium deoxycholate (SDC), 1-propanol and TLC plates with silica gel 60 were purchased from Sigma. Dynamic light scattering data were recorded on a Wyatt DynaPro dynamic light scattering plate reader. The fluorescence spectra were recorded with a QM-4 PTI spectra fluorometer with rhodamine B (3 g/L in CH_3OH) as the standard.

General PI3K Assay

The fluorescent PIP_2 derivative (2 μM, final concentration) was added to the assay buffer (60 μL, final volume) composed of MOPS (50 mM, pH 6.5), NaCl (100 mM), sodium cholate (0.5 mM), DTT (1 mM), $MgCl_2$ (10 mM), and ATP (2 mM). The reaction was initiated by the addition of purified PI3K (2 ng/μL). After incubation at room temperature for the indicated time, the enzymatic reaction was quenched by adding aqueous HCl (2.0 M, 25 μL). The resulting mixture was extracted with $CHCl_3$/MeOH (*v*/*v* = 2:1, 250 μL) for 3 times. The organic layers were separated, combined, and concentrated under vacuum. The resulting residue was re-suspended in $CHCl_3$/MeOH (*v*/*v* = 1:1) for TLC analysis. TLC plates (Merck, Silica Gel-60) were pretreated with a solvent system containing 1.2% potassium oxalate and 1.2 mM EGTA in MeOH/water (*v*/*v* = 2:3) and heated at 110 °C for 20 min before use. The TLC plate was then developed in $CHCl_3$/acetone/MeOH/AcOH/water (*v*/*v*/*v*/*v*/*v* = 40:15:13:12:7) and scanned on a Typhoon 9400 Variable Mode Imager ($\lambda_{ex}/\lambda_{em}$ = 488 nm/520 nm). The fluorescence intensity of different spots on the TLC plate was quantified with ImageQuant software (V.5.0). Alternatively, the reaction mixture was diluted in $CHCl_3$/MeOH (*v*/*v* = 1:1, 10 μL) and spotted on a TLC plate directly for separation and detection.

IC_{50} measurement of PI3K inhibitors

PI3K was incubated with the inhibitors in the assay buffer for 10 min at room temperature before the assay was initiated by the addition of ATP. The final reaction mixture contained: PIP_2 (2 μM for BODIPY-PIP_2 and 4 μM for FL-PIP_2), ATP (20 μM), 2% DMSO, MOPS (50 mM, pH 6.5), NaCl (100 mM), sodium cholate (0.5 mM), DTT (1 mM), $MgCl_2$ (10 mM), and PI3K (2 ng/μL). After incubation at room temperature (90 min for BODIPY-PIP_2, and 180 min for FL-PIP_2), the reaction mixture was diluted with $CHCl_3$/MeOH (*v*/*v* = 1:1) and analyzed as described above.

Capillary electrophoresis

CE analysis of lipid analytes was performed using a custom-built CE system with laser-induced fluorescence detection as previously described [21]. Fused-silica capillaries (40 cm length, 50 μm i.d., 360 μm o.d., Polymicro Technologies, Phoenix, AZ) were used for the analyte separations. A voltage of 16 kV was applied across the capillary during electrophoresis. For CE analysis of the mixtures, sample volumes (0.6 nL) were loaded by hydrodynamic injection. Separation of FL-PIP_2, FL-PIP_3, BODIPY-PIP_2 and BODIPY-PIP_3 was performed in 100 mM Tris, 10 mM SDC, 1 mM $MgCl_2$, 30% 1-propanol, and 5% EOTrol LR, at pH 8.5. Prior to each run, the capillary was flushed with 1 M NaOH for 3 min, deionized H_2O for 3 min, and the separation buffer for 3 min using a pressurized washing system at 20 psi. To directly compare the phosphorylation of reporters with different fluorescent groups, BODIPY-PIP_2 (1 μM) and FL-PIP_2 (1 μM) were reacted with PI3K for 1 h under the conditions described above. The reaction mixture was quenched by adding 1-propanol and the sample was diluted 200-fold in water immediately prior to CE analysis.

3. Results and Discussion

Characterization of FL-PIP_2 and BODIPY-PIP_2

PI3K catalyzes the phosphorylation of the endogenous PIP_2 at the lipid-water interface where the substrate PIP_2 is in the lipid membranes while the phosphate donor ATP is in the aqueous phase [23]. Accordingly, most studies on PI3K reactions have been carried out in lipid vesicles or micelles where the kinetic measurements are complex [11, 24]. Because the fluorescent PIP_2 derivatives have shorter alkyl chains and are relatively more water soluble compared to endogenous PIP_2, we chose to characterize the two probes under soluble conditions. When the lipid substrate was mono-dispersed in the assay buffer, the enzymatic kinetics analysis followed the classical Michaelis-Menton equation. To ensure that the probes did not form micelles under the assay conditions, the critical micelle concentration (CMC), the amphiphile concentration at which the surface tension of the aqueous phase reaches its minimum, was measured for both FL-PIP_2 and BODIPY-PIP_2. The light scattering [25] of different concentrations of BODIPY-PIP_2 and FL-PIP_2 in deionized water at 25 °C was measured and plotted (Fig. 2A). The CMC of FL-PIP_2 was approximately 225 μM while that of BODIPY-PIP_2 was 65 μM. The CMC of endogenous PIP_2 was also measured by this method as 10 μM, which is consistent with the value obtained through other methods reported in the literature [26].

The fluorescence excitation and emission spectra of both BODIPY-PIP_2 and FL-PIP_2 were also measured (Fig. 2B). Both spectra of BODIPY-PIP_2 and FL-PIP_2 are similar as those of the parent fluorophores BODIPY and fluorescein, respectively [27–29]. Compared with FL-PIP_2, BODIPY-PIP_2 possesses a higher extinction coefficient and narrower emission bandwidth. The excitation maximum is 502 nm for BODIPY-PIP_2 and 496 nm for FL-PIP_2, while the emission maximum is 511 nm for BODIPY-PIP_2 and 516 nm for FL-PIP_2. The kinetic measurements of the fluorophore-tagged PIP_2 and PIP_3 in the subsequent experiments were recorded with excitation at 488 nm and detected at 520 nm.

Validation of the PI3K reaction and separation of the reaction mixtures on TLC and CE

The canonical method for detection of PI3K enzymatic activity *in vitro* uses radioactive ATP to incorporate ^{32}P into the reaction product, which is subsequently separated from other components in the reaction mixture on TLC and detected through autoradiography [30–31]. Likewise, we envisioned that the fluorescent PIP_2 derivatives could be used to report PI3K activity by first separating fluorescent PIP_2 from its PI3K reaction product on a TLC plate and then quantifying the ratio of the substrate to product through

fluorescence detection. To optimize the separation efficiency, the TLC plates were pretreated with potassium oxalate and EDTA followed by heating at 110 °C for 20 min. The PI3K reaction mixture was extracted with $CHCl_3$/MeOH (v/v = 2:1) four times and the products were separated on TLC. Under suitable developing solutions (see methods), the BODIPY-PIP_2 and BODIPY-PIP_3 were well separated (Fig. 3A, lane 2). The extraction efficiency, as measured by fluorescence recovery, was approximately 97%. However, it was not clear if BODIPY-PIP_2 and BODIPY-PIP_3 were extracted with the same efficiency, raising concern about the accuracy of the measurement. Moreover, the extraction process was tedious and time-consuming. We thus explored the possibility of analysis without the extraction process. Thus, the reaction mixture was diluted with $CHCl_3$/MeOH (v/v = 1:1) to quench the PI3K-catalyzed reaction and directly separated by TLC (Fig. 3A, lane 3). Interestingly, the separation of BODIPY-PIP_2 from BODIPY-PIP_3 proceeded with almost identical efficiency. Likewise, the FL-PIP_3 was also efficiently separated from FL-PIP_2 on TLC, either with or without the extraction process (Fig. 3B).

We have also attempted to separate a mixture of BODIPY-PIP_2, BODIPY-PIP_3, FL-PIP_2, and FL-PIP_3 on TLC, but did not have success due to the similar Rf values between the FL-tagged and BODIPY-tagged lipids. In contrast, these four fluorescent molecules could be simultaneously measured by CE analysis. As shown in Fig. 3C, a mixture of BODIPY-PIP_2, BODIPY-PIP_3, FL-PIP_2, and FL-PIP_3 were readily separated by CE. We then analyzed an aqueous *in vitro* kinase reaction with PI3K after one hour incubation with both BODIPY-PIP_2 and FL-PIP_2. Under the assay conditions used, 24 ± 5% of FL-PIP_2 and 17 ± 3% of BODIPY-PIP_2 were phosphorylated (n = 5), (Fig. 3D). The difference in phosphorylation of the two fluorescently labeled PIP_2's may be caused by greater loss of the more hydrophobic BODIPY-labeled substrate during sample preparation and incubation thereby reducing its concentration relative to its K_M for PI3K. Under the assay conditions, the detection limits for the fluorescently labeled PIP_2 and PIP_3 were approximately 0.3–1.2 × 10^{-12} for TLC analysis and 1–10 × 10^{-20} mol for CE separation. These are comparable or better than the detection limit (0.5–1 x10^{-12} mol) when the traditional radioactivity-based assay was used.

Kinetics analysis of PI3K activity with fluorescent PIP_2 derivatives

To quantify the kinetic properties of BODIPY-PIP_2 and FL-PIP_2, we measured the K_M and V_{max} of these two probes in the PI3K reaction. To ensure that the measurement was under initial velocity conditions, we explored the effects of reaction time and amount of enzyme on the conversion of BODIPY-PIP_2 (Fig. 4A). When 1.2 ng/μL PI3K was used in the assay, the conversion of BODIPY-PIP_2 was within 10% after 30 min at room temperature while the reaction product could still be easily detected and quantified by fluorescence intensity. These conditions were thus used for subsequent experiments. In the cellular environment, the ATP concentration is in the range of 1–10 mM. The K_M for ATP with endogenous PIP_2 as the substrate is in the range of 20–80 μM [30]. Consequently, we used 2 mM ATP in all the experiments for the K_M and V_{max} measurement.

To carry out the assay, PI3K was added to the assay buffer containing the fluorescent PIP_2 derivative (2 μM) and ATP (2 mM). The concentration of the lipid substrate was varied to generate a series of initial velocities. K_M and V_{max} were then calculated by fitting the data to the Michaelis-Menton equation. Each experiment was carried out in duplicates and repeated three times. The K_M for FL-PIP_2 was 44.8 ± 9.8 μM with a V_{max} of 0.28 ± 0.07 pmol/ng/min (Fig. 4B), while the K_M for BODIPY-PIP_2 was 68.7 ± 5.2 μM with a V_{max} of 1.02 ± 0.33 pmol/ng/min (Fig. 4C).

Measurement of the IC_{50} of PI3K inhibitors using fluorescent PIP_2 derivatives

To test whether this *in vitro* assay system could be used to measure the effects of specific pharmaceutical agents on PI3K activity, the IC_{50} of two known PI3K inhibitors were measured using the two fluorescent PIP_2 derivatives. Both LY294002 and wortmannin are considered to be ATP competitive inhibitors, with LY294002 being reversible and wortmannin irreversible [32–33]. In contrast to the measurement for substrate kinetics where ATP must be saturated, the IC_{50} measurement for ATP competitive inhibitors requires that the ATP concentration is at or below the K_M for ATP. Accordingly, the K_M for ATP was measured when FL-PIP_2 (Fig. 5A) or BODIPY-PIP_2 (Fig. 5B) was used in the PI3K reaction. The $K_{M,\ ATP}$ was 66.9 ± 13.3 μM for FL-PIP_2 and 24.8 ± 4.2 μM for BODIPY-PIP_2, while $V_{max,\ ATP}$ was 3.26 ± 0.22 pmol/μg/min for FL-PIP_2 and 4.72 ± 0.21 pmol/μg/min for BODIPY-PIP_2. Based on these results, 20 μM ATP was used in the reaction mixture to measure the IC_{50} of the PI3K inhibitors.

LY294002 or wortmannin were incubated with PI3K at room temperature for 10 min before the enzyme was added to the assay buffer to initiate the reaction. When FL-PIP_2 was used as the PI3K substrate, the IC_{50} was 1.43 μM for LY294002 and 4.6 nM for wortmannin (Fig. 6A). Both of these values were consistent with those obtained with other methods [32, 34]. Similarly, the IC_{50} for LY294002 and wortmannin (Fig. 6B) were carried out with BODIPY-PIP_2 as the PI3K substrate. The IC_{50} was 1.41 μM and 6.2 nM, respectively.

In summary, we have established an *in vitro* assay system to directly measure PI3K activity. This assay takes advantage of the ready separation of a fluorphore-tagged PIP_2 derivative from its PI3K reaction product on TLC or CE, and the high sensitivity of fluorescence detection. Both FL-PIP_2 and BODIPY-PIP_2 have similar K_M when used as the PI3K substrate, and appear to function equally well to characterize PI3K inhibitors. On the other hand, the V_{max} for BODIPY-PIP_2 is approximately 4-fold greater than that for FL-PIP_2. In addition, the BODIPY-PIP_2 more easily forms micelles, a key character of endogenous PIP_2, than FL-PIP_2 as judged by their CMCs. Finally, the BODIPY fluorophore offers many advantages compared to fluorescein, including a narrow emission bandwidth, spectra that are less sensitive to polarity and pH, longer excited state lifetimes, and a large two-photon cross-section for multiphoton excitation. Taken together, these results suggest that both fluorescent probes are effective PI3K substrates that can be used to measure PI3K activity, but with fine differences. Given the important roles that PI3K plays in cell signaling and disease, this work will facilitate the use of fluorescent PIP_2 derivatives in measuring PI3K activity in cell-based assays, including those using patient samples.

Acknowledgments

We thank the North Carolina University Cancer Research Fund and NIH (CA139599) for financial support.

References

1. Di Paolo G, De Camilli P. Phosphoinositides in cell regulation and membrane dynamics. Nature. 2006; 443:651–657. [PubMed: 17035995]
2. Balla T, Szentpetery Z, Kim YJ. Phosphoinositide signaling: new tools and insights. Physiology (Bethesda). 2009; 24:231–244. [PubMed: 19675354]
3. Castellino RC, Durden DL. Mechanisms of disease: the PI3K-Akt-PTEN signaling node--an intercept point for the control of angiogenesis in brain tumors. Nat Clin Pract Neurol. 2007; 3:682–693. [PubMed: 18046441]
4. Wymann MP, Schneiter R. Lipid signalling in disease. Nat Rev Mol Cell Biol. 2008; 9:162–176. [PubMed: 18216772]

5. Liu ZN, Roberts TM. Human tumor mutants in the p110 alpha subunit of PI3K. Cell Cycle. 2006; 5:675–677. [PubMed: 16627990]
6. Comprehensive genomic characterization defines human glioblastoma genes and core pathways. Nature. 2008; 455:1061–1068. [PubMed: 18772890]
7. Yuan TL, Cantley LC. PI3K pathway alterations in cancer: variations on a theme. Oncogene. 2008; 27:5497–5510. [PubMed: 18794884]
8. Liu P, Cheng H, Roberts TM, Zhao JJ. Targeting the phosphoinositide 3-kinase pathway in cancer. Nat Rev Drug Discov. 2009; 8:627–644. [PubMed: 19644473]
9. Courtney KD, Corcoran RB, Engelman JA. The PI3K pathway as drug target in human cancer. J Clin Oncol. 2010; 28:1075–1083. [PubMed: 20085938]
10. Workman P, Clarke PA, Raynaud FI, van Montfort RL. Drugging the PI3 kinome: from chemical tools to drugs in the clinic. Cancer Res. 2010; 70:2146–2157. [PubMed: 20179189]
11. Fruman DA, Meyers RE, Cantley LC. Phosphoinositide kinases. Annu Rev Biochem. 1998; 67:481–507. [PubMed: 9759495]
12. Hsu FF, Turk J. Characterization of phosphatidylinositol, phosphatidylinositol-4-phosphate, and phosphatidylinositol-4,5-bisphosphate by electrospray ionization tandem mass spectrometry: A mechanistic study. J Am Soc Mass Spectr. 2000; 11:986–999.
13. Wenk MR, et al. Phosphoinositide profiling in complex lipid mixtures using electrospray ionization mass spectrometry. Nat Biotechnol. 2003; 21:813–817. [PubMed: 12808461]
14. Balla T, Varnai P. Visualizing cellular phosphoinositide pools with GFP-fused protein-modules. Sci STKE. 2002; 2002:pl3. [PubMed: 11917154]
15. Gray A, Olsson H, Batty IH, Priganica L, Downes CP. Nonradioactive methods for the assay of phosphoinositide 3-kinases and phosphoinositide phosphatases and selective detection of signaling lipids in cell and tissue extracts. Anal Biochem. 2003; 313:234–245. [PubMed: 12605860]
16. Drees BE, et al. Competitive fluorescence polarization assays for the detection of phosphoinositide kinase and phosphatase activity. Comb Chem High T Scr. 2003; 6:321–330.
17. Taylor GS, Dixon JE. An assay for phosphoinositide phosphatases utilizing fluorescent substrates. Anal Biochem. 2001; 295:122–126. [PubMed: 11476556]
18. Zhong W, Murphy DJ, Georgopapadakou NH. Inhibition of yeast inositol phosphorylceramide synthase by aureobasidin A measured by a fluorometric assay. FEBS Lett. 1999; 463:241–244. [PubMed: 10606729]
19. Ozaki S, DeWald DB, Shope JC, Chen J, Prestwich GD. Intracellular delivery of phosphoinositides and inositol phosphates using polyamine carriers. Proc Natl Acad Sci U S A. 2000; 97:11286–11291. [PubMed: 11005844]
20. Borland LM, Kottegoda S, Phillips KS, Allbritton NL. Chemical analysis of single cells. Annu Rev Anal Chem (Palo Alto Calif). 2008; 1:191–227. [PubMed: 20636079]
21. Mwongela SM, Lee K, Sims CE, Allbritton NL. Separation of fluorescent phosphatidyl inositol phosphates by CE. Electrophoresis. 2007; 28:1235–1242. [PubMed: 17366487]
22. Chen J, Profit AA, Prestwich GD. Synthesis of Photoactivatable 1,2-O-Diacyl-sn-glycerol Derivatives of 1-L-Phosphatidyl-D-myo-inositol 4,5-Bisphosphate (PtdInsP(2)) and 3,4,5-Trisphosphate (PtdInsP(3)). J Org Chem. 1996; 61:6305–6312. [PubMed: 11667472]
23. Barnett SF, et al. Interfacial catalysis by phosphoinositide 3′-hydroxykinase. Biochemistry. 1995; 34:14254–14262. [PubMed: 7578025]
24. Carson JD, et al. Effects of oncogenic p110alpha subunit mutations on the lipid kinase activity of phosphoinositide 3-kinase. Biochem J. 2008; 409:519–524. [PubMed: 17877460]
25. Tsamaloukas AD, Beck A, Heerklotz H. Modeling the micellization behavior of mixed and pure n-alkyl-maltosides. Langmuir. 2009; 25:4393–4401. [PubMed: 19366219]
26. Walsh JP, Suen R, Glomset JA. Arachidonoyl-diacylglycerol kinase. Specific in vitro inhibition by polyphosphoinositides suggests a mechanism for regulation of phosphatidylinositol biosynthesis. J Biol Chem. 1995; 270:28647–28653. [PubMed: 7499383]
27. Strandberg L, et al. Fluorescence studies on plasminogen activator inhibitor 1: reactive centre cysteine mutants remain active after fluorophore attachment. Thromb Res. 1994; 76:253–267. [PubMed: 7863476]

28. Klonis N, Sawyer WH. Effect of solvent-water mixtures on the prototropic equilibria of fluorescein and on the spectral properties of the monoanion. Photochem Photobiol. 2000; 72:179–185. [PubMed: 10946570]

29. Schauenstein K, Schauenstein E, Wick G. Fluorescence properties of free and protein bound fluorescein dyes. I. Macrospectrofluorometric measurements. J Histochem Cytochem. 1978; 26:277–283. [PubMed: 77868]

30. Carpenter CL, et al. Purification and characterization of phosphoinositide 3-kinase from rat liver. J Biol Chem. 1990; 265:19704–19711. [PubMed: 2174051]

31. Carpenter CL, Cantley LC. Phosphoinositide kinases. Biochemistry. 1990; 29:11147–11156. [PubMed: 2176895]

32. Vlahos CJ, Matter WF, Hui KY, Brown RF. A specific inhibitor of phosphatidylinositol 3-kinase, 2-(4-morpholinyl)-8-phenyl-4H-1-benzopyran-4-one (LY294002). J Biol Chem. 1994; 269:5241–5248. [PubMed: 8106507]

33. Vanhaesebroeck B, et al. Synthesis and function of 3-phosphorylated inositol lipids. Annu Rev Biochem. 2001; 70:535–602. [PubMed: 11395417]

34. Wymann MP, et al. Wortmannin inactivates phosphoinositide 3-kinase by covalent modification of Lys-802, a residue involved in the phosphate transfer reaction. Mol Cell Biol. 1996; 16:1722–1733. [PubMed: 8657148]

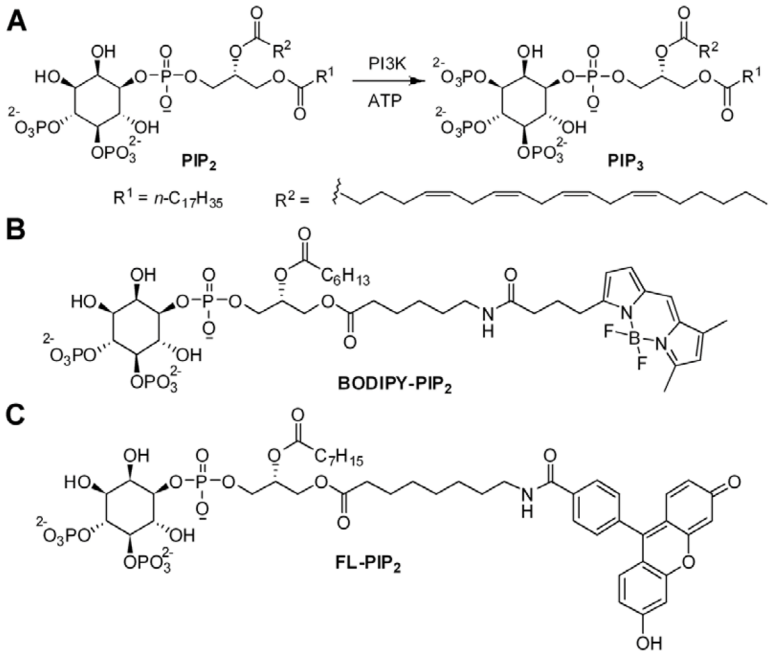

Figure 1.

Schematic illustration of the PI3K reaction. **A.** the endogenous PIP_2 is phosphorylated at the 3′-OH to form PIP_3; **B, C.** Chemical structures of fluorescent PIP_2 derivatives BODIPY-PIP_2 (**B**) and FL-PIP_2 (**C**).

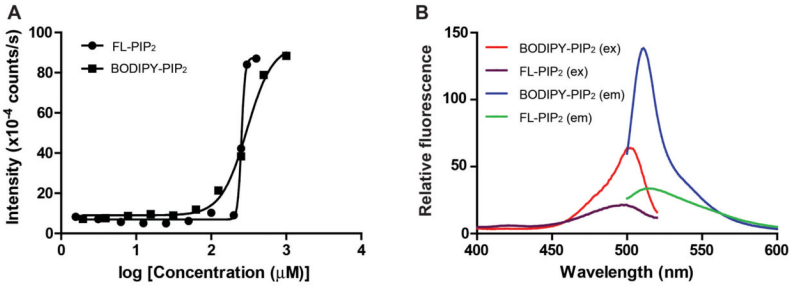

Figure 2.

Biophysical characterization of FL-PIP_2 and BODIPY-PIP_2. **A.** Measurement of critical micelle concentrations (CMCs) of FL-PIP_2 and BODIPY-PIP_2. **B**. Fluorescence excitation and emission spectra of FL-PIP_2 and BODIPY-PIP_2.

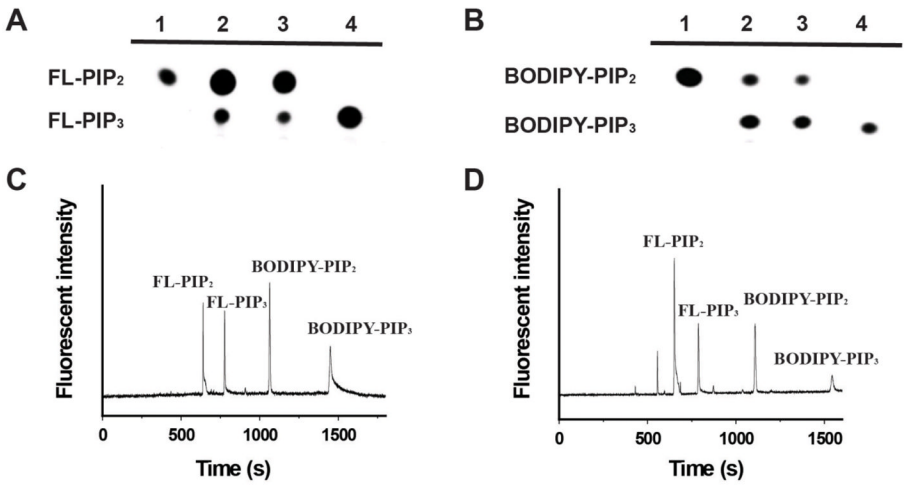

Figure 3.

Separation of the PI3K reaction mixtures with fluorescent PIP_2 derivatives through TLC or CE analysis. **A.** the separation of the reaction mixture of FL-PIP_2 on TLC. lane 1: FL-PIP_2; lane 2: the reaction mixture was extracted with $CHCl_3$/MeOH (*v*/*v* = 2:1) before TLC separation; lane 3: the reaction mixture was diluted with $CHCl_3$/MeOH (*v*/*v* = 1:1) and separated on TLC; lane 4: FL-PIP_3. **B.** the separation of the reaction mixture of BODIPY-PIP_2 on TLC. lane 1: BODIPY-PIP_2; lane 2: the reaction mixture was extracted with $CHCl_3$/MeOH (*v*/*v* = 2:1) before TLC separation; lane 3: the reaction mixture was diluted with $CHCl_3$/MeOH (*v*/*v* = 1:1) and separated on TLC; lane 4: BODIPY-PIP_3. **C.** The separation of a mixture of FL-PIP_2, FL-PIP_3, BODIPY-PIP_2, and BODIPY-PIP_3 by CE; **D.** A 1:1 mixture of FL-PIP_2 and BODIPY-PIP_2 were used for the PI3K reaction, and the reaction mixture was separated by CE.

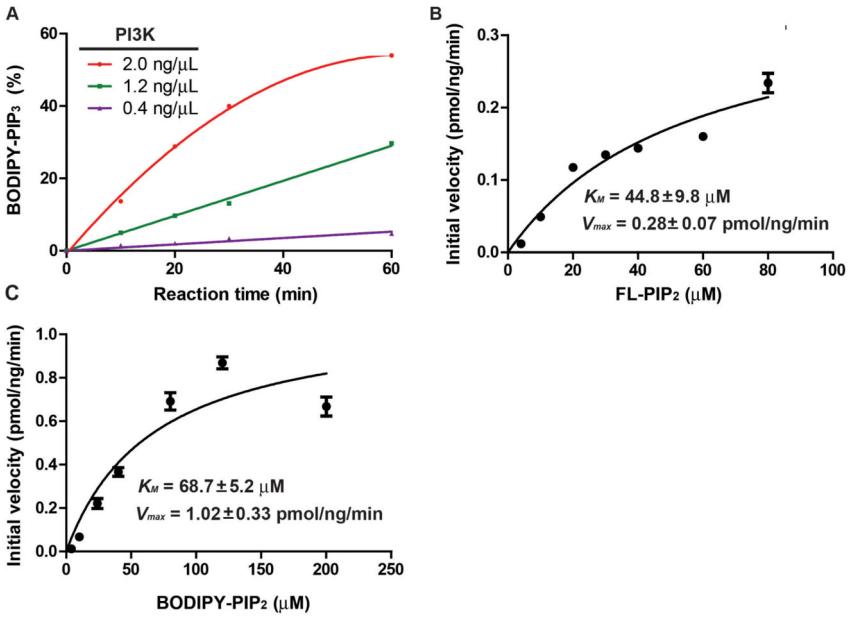

Figure 4.

Kinetic analysis of PI3K reaction with fluorescent PIP_2 derivatives. **A.** The reaction progress curves with different amounts of PI3K were used. **B.** Kinetic studies on PI3K reaction with FL-PIP_2. **C.** Kinetic studies on PI3K reaction with BODIPY-PIP_2. Each experiment was carried out in duplicate and repeated three times.

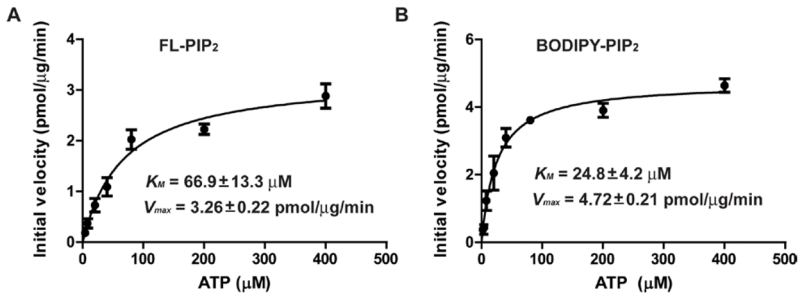

Figure 5.

Measurement of K_M for ATP for the PI3K reactions with FL-PIP_2 (**A**) or BODIPY-PIP_2 (**B**) as the lipid substrate. Each experiment was carried out in duplicate and repeated three times.

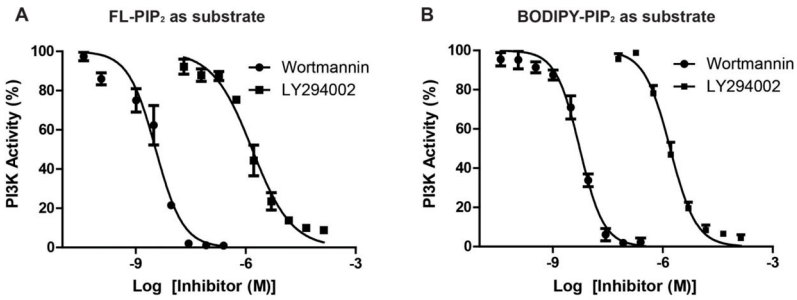

Figure 6.

Dose response curves of PI3K inhibitors LY294002 and wortmannin. **A.** IC_{50} values of LY294002 and wortmannin were measured with FL-PIP_2 as the PI3K substrate; **B.** IC_{50} values of LY294002 and wortmannin were measured with BODIPY-PIP_2 as the PI3K substrate. Each experiment was carried out in duplicate and repeated three times.